Solid-State NMR Investigation of Morphology in Poly(*N*-vinylcarbazole) Complexes with Poly(ethylene glycol) Monomethyl Ether 3,5-Dinitrobenzoate

G. Cojocariu* and A. Natansohn

Department of Chemistry, Queen's University, Kingston, Ontario K7L 3N6, Canada

Received December 29, 2002; Revised Manuscript Received February 2, 2003

ABSTRACT: Interactions and morphology were investigated by solid-state NMR in macromolecular charge transfer (CT) complexes formed between poly(*N*-vinylcarbazole) (PVK) and a surfactant consisting of a monomethyl ether poly(ethylene glycol) (PEG) oligomer functionalized at one end with a 3,5-dinitrobenzoyl (DNB) group. ^{13}C CP MAS NMR spectra indicated that in the PVK/PEG−DNB complexes containing 33.1 and 50.0 mol % PEG−DNB, the PEG chains undergo microphase separation. The balance between the PVK/DNB CT interactions and the repulsion between the PVK backbone and the PEG side chains produces comblike structures similar to those observed in polyelectrolyte/surfactant complexes. The size of the domains in these microphase-separated comblike CT complexes was evaluated on the basis of proton spin−lattice relaxation time in the rotating frame [$T_{1\rho}$(H)] and spin diffusion data. Assuming a lamellar morphology, the PEG microdomain is about 3 nm thick. The size of the PVK/DNB microdomains was estimated at about 5 nm, suggesting that the PVK chains must be oriented perpendicular to the direction of the domain thickness, in the layer plane, the layer thickness being given by about two to three PVK chains.

Introduction

Because of their ability to form various morphologies with sizes ranging from few to tens of nanometers, segmented copolymers containing dissimilar blocks have been intensively studied as structure-controlled nanomaterials.[1,2] As opposed to blends of incompatible homopolymers that are usually phase separated at a macroscopic level, in segmented copolymers macrophase separation is prevented by the chemical connectivity of the constituent blocks, which leads to microphase-separated structures. In macrophase-separated blends the domain sizes normal and parallel to the interface are much larger than the size of the individual polymer chains. On the other hand, in microphase-separated copolymers the domain size normal to the interface is comparable to the size of the individual blocks.

Replacing the covalent bonds between the constituent blocks with noncovalent interactions has emerged as a new and versatile approach toward nanostructured materials. Once the "building block" molecules, capable of secondary interactions, are synthesized, a variety of supramolecular architectures can be easily obtained simply by mixing these molecules in a common solvent followed by precipitation or film casting. Solid comblike or "bottle brush" complexes have been intensively studied lately in polyelectrolyte/surfactant mixtures due to their potential as facile building blocks for self-organizing materials.[4−20] To obtain microphase-separated noncovalent polymer brushes, one has to fulfill two important requirements.[12] One requirement is to have sufficiently strong noncovalent interactions, such as ionic,[7,16−18] hydrogen bonding[4,9−15] or metal coordination,[19−20] that bind one end group of the side chain to the polymer backbone. These interactions prevent macrophase separation in a similar way the covalent connectivity does in block copolymers. The second requirement is to have a certain amount of repulsion between the rest of the side chain and the backbone, so that the two parts undergo microphase separation at a nanometer scale. If the repulsion is too strong, macrophase separation may occur, while if the repulsion is too weak, the side chains and backbone will be randomly mixed.

Organic charge transfer (CT) complexes[21,22] can be used as binding forces to promote compatibility in polymer blends.[23,24] This paper studies macromolecular charge transfer complexes formed between poly(*N*-vinylcarbazole) (PVK) and a surfactant that has been investigated previously,[25,26] poly(ethylene glycol) monomethyl ether 3,5-dinitrobenzoate, (PEG−DNB). The purpose of studying these complexes is to test their ability to form polymer comblike structures, the hypothesis being that PEG−DNB molecules will attach as side chains to PVK backbone, through CT complexation of the carbazole from PVK with the DNB end group from PEG−DNB (Figure 1). To our knowledge, this is the first report of using aromatic $\pi-\pi$ CT complexation as the binding force in polymer/surfactant complexes. In balance to CT binding forces, the repulsive interactions between PVK backbone and PEG side chains are expected to render microphase separation.

To investigate the interactions and morphology in these complexes, solid-state NMR was employed as the main tool. High-resolution solid-state NMR is a very powerful tool for investigation of polymer dynamics and microphase structure in multicomponent polymer systems.[27−40] One of the most often used spin relaxation methods to characterize polymers in solid state is proton spin−lattice relaxation in the rotating frame, $T_{1\rho}$(H). The number of relaxation time constants can be associated with the number of phases in a mixture and therefore gives information about miscibility in multicomponent polymer systems.[27,28,36−40] The presence of spin diffusion during the spin relaxation process tends to average the measured $T_{1\rho}$(H) in systems where the heterogeneities are smaller than a few nanometers, which is the resolution limit for phase structure investigation by this method.[28] Probably the most powerful

10.1021/ma026012h CCC: $25.00
Published on Web 03/11/2003

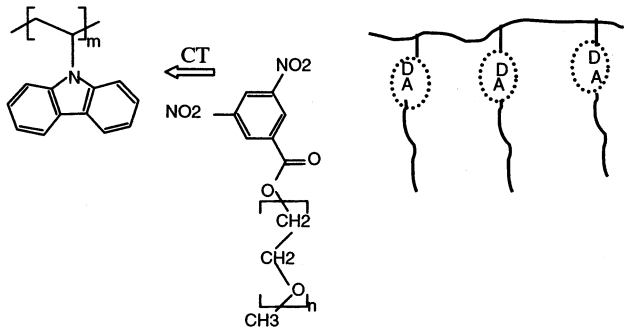

Figure 1. Comblike complexes to be formed by PVK and PEG−DNB. PEG side chains are bound to the PVK backbone by CT complexation between the carbazole donor (D) and DNB acceptor (A).

NMR method in studying morphology in multicomponent polymer systems is the technique called spin diffusion, based on selective excitation of one phase followed by monitoring magnetization transfer until the system reaches equilibrium. Pulse sequence filters can be designed to discriminate between microphases using differences in chemical shifts[29] or mobility.[30] The analysis of the spin diffusion data provides information about phase structure and microdomain sizes down to 0.5 nm.[29−34]

Experimental Section

Materials and Sample Preparation. Poly(*N*-vinylcarbazole) (PVK) (Aldrich, 10^6 g/mol) was precipitated three times in methanol from tetrahydrofuran (THF) solutions. The synthesis of poly(ethylene glycol) monomethyl ether 3,5-dinitrobenzoate (PEG−DNB) was described elsewhere.[25] The weight-average molecular weight of PEG−DNB is 560 g/mol.[25] Poly(ethylene glycol) monomethyl ether, PEG (Aldrich, 350 g/mol), and PEG−DNB were dried under vacuum at 40 °C for 2 days before use. PVK mixtures with PEG−DNB or PEG were prepared by dissolving both components in THF at relatively low concentration (about 1 wt %) followed by slow evaporation of the solvent. The samples were then kept in a vacuum oven at 40 °C for at least 2 days and subsequently stored in a desiccator. A few samples were also cast from chloroform to see whether there is any solvent effect. DSC and NMR relaxation time measurements showed similar results for both solvents. The mol % concentrations refer to moles of PEG−DNB chains and moles of *N*-vinylcarbazole repeating units.

Solid-State NMR. The solid-state NMR experiments were performed at room temperature on a Bruker ASX-200 spectrometer operating at 200 and 50.29 MHz for ^{1}H and ^{13}C, respectively. ^{13}C detection was achieved through cross-polarization (CP), magic angle spinning (MAS), and dipolar decoupling (DD). The $\pi/2$ pulse length was 4.7 μs (spin-locking field frequency of 53 kHz). An optimum contact time of 1 ms was used for all measurements, except for the pure PVK sample, for which a contact time of 5 ms was used. For the 1D ^{13}C CP MAS experiments samples were spun at 6.3 kHz, except for the sample containing 50.0 mol % PEG−DNB that, for packing reasons, was spun at 5.0 kHz. For all the other experiments spinning at 5.0 kHz was employed. Measurements of proton relaxation time in the rotating frame, $T_{1\rho}$(H), were done using ^{13}C detection. After a variable spin-locking time the proton magnetization is transferred to carbon nuclei during a constant cross-polarization time. ^{1}H spin diffusion measurements were performed using a dipolar filter sequence.[30] The delay between the 12 $\pi/2$ pulses applied during the filter was 11 μs, and the pulse train was cycled five times for each scan. Phase cycling (PC, π pulse between the dipolar filter and the mixing time at every other scan) was used to minimize the effect of proton spin−lattice relaxation time in the laboratory frame (T_1). The dipolar filter sequence is shown in Figure 2.

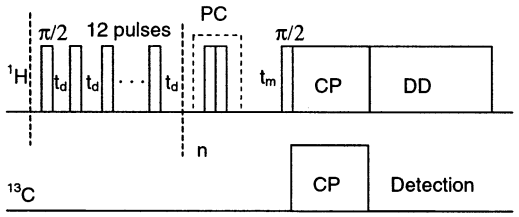

Figure 2. Pulse sequence for dipolar filter experiments.

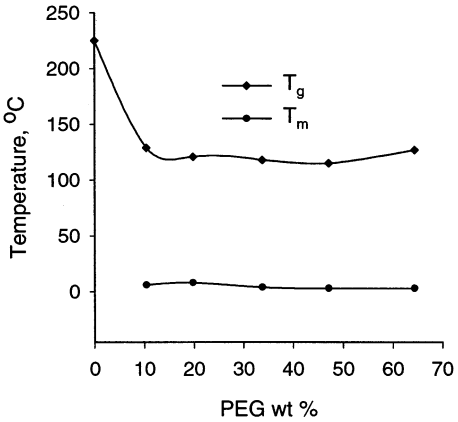

Figure 3. Glass transition (T_g) and melting (T_m) temperatures in mixtures of PVK/PEG.

UV−vis Spectroscopy. Electronic spectra were recorded on a Hewlett-Packard 8452A diode array ultraviolet−visible spectrophotometer at room temperature. For solid samples films of 50 μm thickness were cast on quartz plates. For liquid PEG−DNB a thin (1 mm) quartz cuvette was used. The data were not corrected for thickness since the strong CT transition was already evident even in films much thinner than the cuvette containing the PEG−DNB acceptor.

Thermal Characterization. DSC thermograms were recorded on the second heating with a Perkin-Elmer DSC 6 instrument, under a nitrogen atmosphere, at a heating rate of 20 °C/min, on the same samples that were used for solid-state NMR. Samples were scanned from −80 to +250 °C.

Results and Discussion

DSC Studies. The glass transition temperature (T_g) is often used to investigate miscibility and homogeneity in multicomponent polymer systems. Usually, the presence of a single T_g can be used to support homogeneity down to the level of a freely jointed chain, whose motion onset is at the glass transition temperature. On the basis of this, T_g measurements are considered to be sensitive to phase sizes greater than about 15 nm.[41] Using T_g as a criterion for polymer miscibility requires that the values for the T_g of the components in pure state be well separated, so that DSC or any other method can discriminate between the component transitions.

Mixtures of PVK and unmodified poly(ethylene glycol) (PEG) were tested first. These samples were all macrophase-separated, forming cloudy and brittle films. Cloudiness indicates the existence of heterogeneous domains having sizes comparable to the visible light wavelength. At high PEG load, the samples had a greasy aspect from the PEG that exuded out of the film. The two-phase structure is supported by the two thermal transitions observed for PVK/PEG mixtures of different compositions (Figure 3). All samples had an amorphous phase, rich in PVK, and characterized by a glass transition (T_g), and a crystalline phase made of excess PEG and characterized by a melting transition

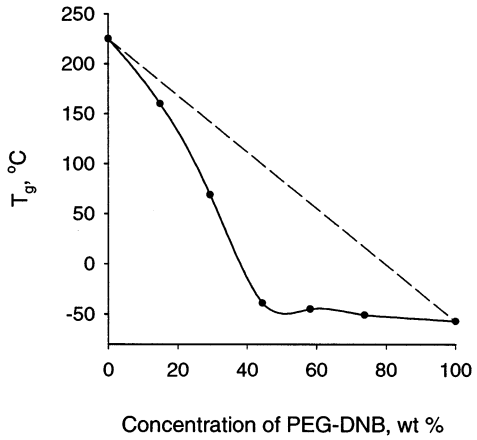

Figure 4. Composition dependence of the single glass transition in miscible PVK/PEG−DNB mixtures. Dotted line represents the weighted average values for T_g.

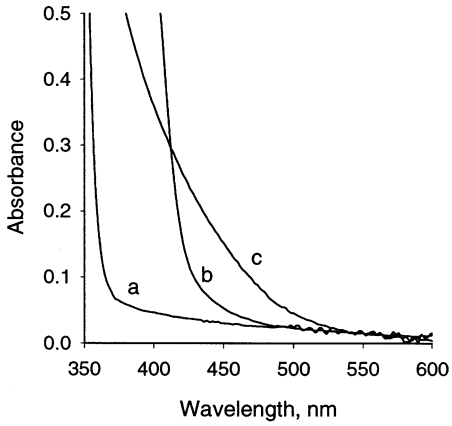

Figure 5. UV−vis spectra for (a) PVK, (b) PEG−DNB, and (c) PVK/PEG−DNB complex having 33.1 mol % PEG−DNB. See Experimental Section for sample details.

(T_m). The T_g of the amorphous phase dropped significantly when 10 wt % PEG was added but did not change as the amount of PEG was increased from 10 to 65 wt %. The initial drop in T_g indicates that PVK mixes intimately with small amounts of PEG. The concentration independence of T_g at PEG concentrations higher than 10 wt % means that the amorphous phase composition does not change with the overall composition. This is common for a phase-separated system, where adding more of one component changes the volume fraction of the separated phases but does not change their composition.[42] The data suggest that mixing of PVK and PEG result in incompatible phases, at least in the concentration range investigated here. This is relevant for the objective of obtaining PVK/PEG−DNB comblike complexes, since some incompatibility between PVK and PEG phases is required for microphase separation to occur.

For the mixtures of PVK with PEG−DNB all samples showed a single thermal transition, namely a glass transition. It should be mentioned that pure PEG−DNB has a glass transition at −57 °C and no melting transition. The properties of PEG−DNB itself were further addressed elsewhere.[26] The T_g values for the PVK/PEG−DNB mixtures were in the range given by the values observed for the pure components, PVK (225 °C) and PEG−DNB (−57 °C), and decreased significantly with increasing the concentration of PEG−DNB (Figure 4). This proves that PVK and PEG−DNB form homogeneous mixtures down to at least 15 nm. The increase in compatibility indicates that the presence of a DNB group promotes some favorable interactions between PVK and PEG−DNB. These interactions are most likely CT interactions between the carbazole and the DNB, and they are also very relevant for the investigated polymer combs, since they provide the binding forces between backbone and side chains. The CT complexation between DNB and carbazole is supported by the extra absorbance that appears at 430−530 nm in the UV−vis spectra when PVK is mixed with PEG−DNB (Figure 5).

It is clear in Figure 4 that PEG−DNB acts as a very good plasticizer for the rigid PVK, turning it from a rigid plastic (T_g = 225 °C) to a rubbery material (T_g = −50 to −40 °C) at high concentrations of the oligomer. The concentration dependence of the glass transition temperature in Figure 4 shows a negative deviation from the weighted average of the two components. Qualitatively, a positive deviation for the T_g of the mixture from the weighted average of the T_g's of its pure components is associated with strong intermolecular interactions between the components.[23,44,45] These interactions act as cross-links to reduce the mobility and the free volume of the mixture and therefore raise the T_g. Negative deviations, on the other hand, are associated with an excess in the free volume over the weighted average value.[46−49] In the PVK/PEG−DNB system, the very mobile PEG chains cause a significant increase in free volume around the PVK chain. The PVK/DNB CT interactions keep the mobile PEG chains close to the PVK backbone where they replace the rigid neighboring PVK chains. The repulsion between the PEG chains and the PVK backbone is also a factor that contributes to the high free volume. The negative deviation of T_g seems to be a common feature for rigid polymers that form strong interactions with flexible oligomers through the oligomer end groups. Poly(*N*-vinylpyrrolidone) (PVP) plasticized with PEG oligomers of certain molecular weights[47−49] showed T_g's significantly lower than the weighted averages of the values corresponding to the two components. The miscibility between the rigid PVP and the flexible PEG is promoted by hydrogen bonding between the hydroxyl end groups from PEG and carbonyl groups from PVP.[50] In the absence of hydrogen bonding PVP is immiscible with oxyethylene derivatives.[50,51] The key point, in the case presented here and the reports from the literature,[47−50] is that, although the oligomers develop strong interactions to the polymer backbone by either CT or hydrogen bonding to their end groups, they also have repulsive interactions between their chains and the polymer backbone. These repulsive interactions together with the high mobility of the oligomer chains cause the excess of free volume responsible for the significant negative deviation of T_g.

^{13}C CP MAS NMR Spectra. Figure 6 shows ^{13}C CP MAS spectra for PVK and a series of its complexes with increasing amounts of PEG−DNB. The group of large peaks between 100 and 150 ppm corresponds to the aromatic carbons from PVK. The peaks of the DNB carbons are overlapped by the downfield peak of the carbazole and become visible (150 and 160 ppm) only at high concentrations of PEG−DNB. The peak at 70 ppm corresponds to the methylene carbons from the PEG chains. It is this peak that gives us some information about the PVK/PEG−DNB complex. At low concentrations of the surfactant, the PEG peak is broad,

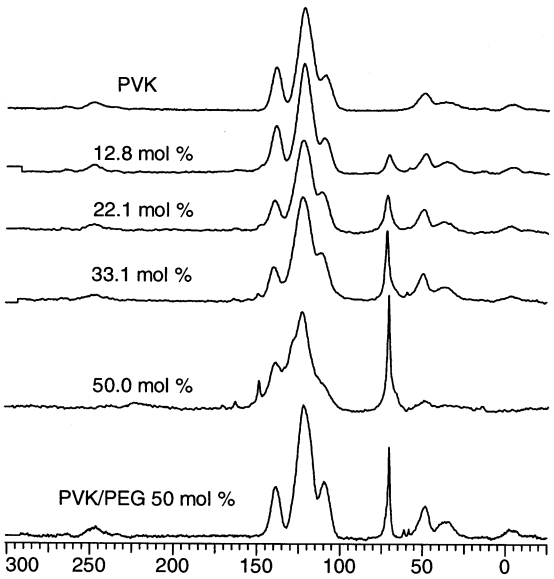

Figure 6. ^{13}C CP MAS of PVK and its mixtures with different concentrations of PEG−DNB (mol % given on the spectrum) and PEG.

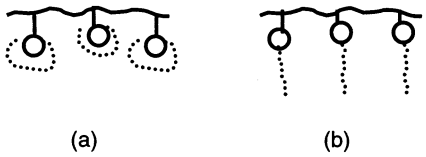

Figure 7. Schematic representation of PVK/PEG−DNB complexes: (a) PEG chains remain coiled around DNB and (b) PEG chains undergo microphase separation. Solid circles represent the carbazole/DNB complex; solid and dotted lines are PVK backbone and PEG chains, respectively.

which is an indication for a rigid local environment of the PEG chains. It was observed previously that the DNB group is able to form intramolecular complexes with its own PEG chain coiled around, in a sidewise position to the aromatic ring.[25,26] When *N*-ethylcarbazole (NEK) was solubilized in aqueous solutions of PEG−DNB, dual complexes with both carbazole and PEG at the same time were formed, with carbazole donors located below and above the DNB ring, in a coplanar symmetric sandwich configuration, where they are not interfering with the PEG chains.[43] It is very likely that in the PVK/PEG−DNB complexes, at low concentrations of PEG−DNB, the PEG chains are still coiled around the DNB group, which is itself complexed to the rigid carbazole groups. PEG chains in such a structure (Figure 7a) are expected to be pretty rigid.

On adding more surfactant, the PEG methylene carbons develop a sharp peak, which is resembling the sharp peak that is seen for unmodified PEG in its macrophase-separated mixtures with PVK (Figure 6, bottom). The sharp peak indicates the presence of PEG chains in a mobile environment. This is not unexpected, since an increase in flexibility with the amount of oligomer has been already seen from DSC. In addition, by increasing the oligomer concentration, the PEG chains may undergo microphase separation, removing themselves from around the rigid PVK/DNB complex (Figure 7b). This microphase separation is probably also the reason for the high free volume (very low T_g, Figure 4) observed in mixtures with high load of PEG−DNB.

Although the PEG peaks are predominantly sharp at 33.1 and 50 mol % PEG−DNB, they are still accompanied by a small broad component, which can be seen at the base of the sharp peaks, slightly shifted upfield (Figure 8). This broadness is not observed in any of the samples containing unmodified PEG. The plot of normalized areas of the sharp and broad component of the PEG peak vs contact time is shown in Figure 9 for a sample containing 33.1 mol % PEG−DNB. Similar behavior was observed for the sample containing 50 mol % PEG−DNB, while the deconvolution was less straightforward with samples that have lower concentrations of the surfactant. The broad component reaches maximum magnetization much faster (1 ms) than the sharp component (5 ms). The difference in cross-polarization efficiency between the two peak components reflects the mobility difference between the corresponding methylene groups. The high cross-polarization efficiency observed for the broad component indicates that these methylene groups are less mobile than the methylene groups that produce the sharp component. The presence of the methylene groups with different mobilities is probably caused by the molecular weight polydispersity of PEG−DNB. Shorter PEG chains have a weaker tendency to microphase separate, and they are probably relatively close to the PVK/DNB rigid complex, maybe still coiled around the DNB group (Figure 7a), experiencing a more rigid environment than the longer and microphase separated chains (Figure 7b). The proximity of the shorter chains to the aromatic rings of the complex is also suggested by the upfield shift of the broader signal, which is probably the result of shielding from the DNB and carbazole ring currents. This effect is somehow similar to the molecular weight resolution observed in solution proton NMR spectra.[25,26]

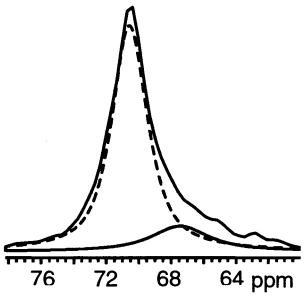

Figure 8. Deconvolution of the PEG peak in the ^{13}C CP MAS spectrum of the PVK/PEG−DNB mixture containing 33.1 mol % PEG−DNB.

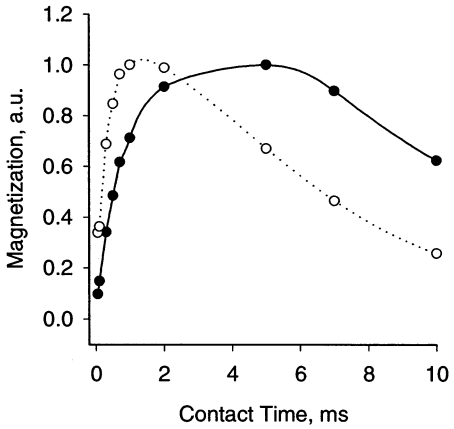

Figure 9. Plot of the normalized areas for the broad (○) and sharp (●) component of the PEG peak (see Figure 8) as a function of the contact time.

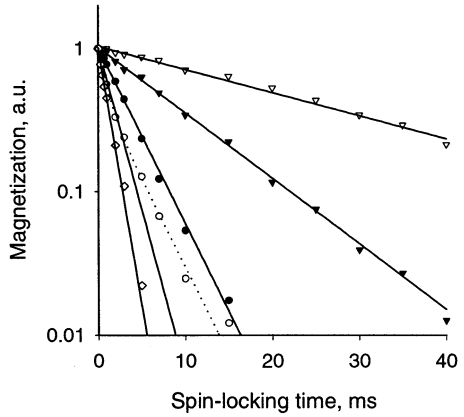

Figure 10. PEG signal decay in $T_{1\rho}$(H) experiments done on PVK mixtures with different concentrations of PEG−DNB: 5.9 (▽), 12.8 (▼), 22.1 (○), 33.1 (●), and 50.0 mol % (◊). Solid lines represent monoexponential fits.

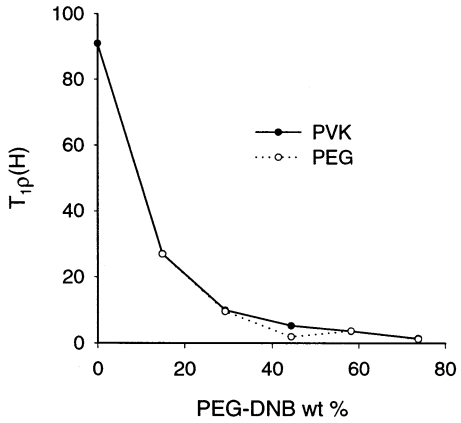

Figure 11. Composition dependence of $T_{1\rho}$(H).

Rotating Frame Spin−Lattice Relaxation Time. Further information about the chain dynamics and phase structure comes from measuring NMR relaxation times, such as proton spin−lattice relaxation time in the rotating frame, $T_{1\rho}$(H). $T_{1\rho}$(H) values are mainly determined by dipolar interaction, which is related to molecular motion in the kilohertz range and interproton distance in the sample.[28] They can be used to characterize miscibility and phase structure in multicomponent polymer systems in a similar way to T_g but are able to detect inhomogeneity down to a few nanometers.[27,28] Samples that are homogeneous down to that level and below will show a single $T_{1\rho}$(H) that is averaged by the fast spin diffusion process between the small domains.

For the $T_{1\rho}$(H) experiments performed in this work, proton magnetization was transferred through cross-polarization to ^{13}C nuclei, which were then used for detection. The $T_{1\rho}$(H) relaxation for the aromatic signal of PVK was monoexponential for all the PVK/PEG−DNB complexes, indicating that PVK is homogeneously dispersed. Figure 10 shows the PEG magnetization decay during $T_{1\rho}$(H) experiments done on PVK/PEG−DNB mixtures of different composition. The relaxation behavior for most of the samples is monoexponential, indicating homogeneous distribution of the PEG−DNB molecules. However, for the sample having 22.1 mol % PEG−DNB, the PEG signal decay shows a deviation from a monoexponential behavior and is faster than in a sample containing 33.1 mol % PEG−DNB (Figure 10). This observation suggests that some sort of inhomogeneity is present in the PEG−DNB component of the 22.1 mol % mixture. This behavior was reproducible on repreparing the corresponding sample and repeating the measurements. One explanation may be that the weight concentration in this sample is 44.4% PEG−DNB, which means that the volume fractions of the two components, PVK and PEG−DNB, are about 0.5. For entropic reasons, in polymer mixtures, the highest tendency for phase separation is observed when the volume fraction of the two components is close to 0.5, or the mixture is symmetric.[42] Probably, in the 22.1 mol % mixture, some of the PEG−DNB is phase-separated, at a scale in between a few nanometers (biexponential $T_{1\rho}$(H) relaxation) and about 15 nm (single T_g). Fitting a biexponential equation to the PEG signal in the 22.1 mol % mixture, two relaxation times can be calculated. One is 3.6 ms and is relatively close to the 5.4 value that was observed for PVK in the same mixture. The second $T_{1\rho}$(H) is about 0.8 ms, the shortest seen for any sample, and significantly different from the PVK value. It is very likely that the 3.6 ms relaxation time corresponds to PEG−DNB bound to PVK, while the short $T_{1\rho}$(H) corresponds to phase-separated PEG−DNB.

In Figure 11 the composition dependence of $T_{1\rho}$(H) in PVK/PEG−DNB complexes is given. The similar values obtained for PVK and PEG−DNB suggest that PVK/PEG−DNB complexes are homogeneous down to a few nanometers. $T_{1\rho}$(H) decreased significantly with increasing the concentration of PEG−DNB. A similar behavior was observed for T_g (Figure 4) due to an increase in the mobility of the sample with the amount of PEG−DNB. The fact that relaxation becomes faster in more mobile samples indicates that the motion regime in the investigated samples is on the low-temperature side ("solid" regime) of the minimum in the plot of spin−lattice relaxation time vs 1/temperature.[52] The negative deviation from a linear dependence is probably due to the short interproton distance within the binding carbazole/DNB complexes. The only sample for which $T_{1\rho}$(H) was different for the PVK and PEG signal was the sample at 22.1 mol %.

Spin Diffusion Analysis. On the basis of the single values found for T_g and $T_{1\rho}$(H), the samples investigated here appear to be homogeneous down to segmental level. However, ^{13}C CP MAS spectra suggest that the PEG chains undergo microphase separation from the PVK backbone. The size of the microdomains must be very small, of the order of few nanometers, since the $T_{1\rho}$(H) is averaged by spin diffusion, except for the 22.1 mol % sample. To clearly define the microphase separation and to determine the size of the microdomains, spin diffusion NMR with a dipolar filter[30] was employed.

The dipolar filter pulse sequence (Figure 2) is used to create a magnetization gradient between the PVK and PEG microphases. The dipolar filter requires a difference in mobility between the two components. The more rigid component, with stronger dipolar interactions, has its magnetization suppressed, while the magnetization of the mobile component is preserved and its transfer to the rigid phase is monitored as spin diffusion. Here PVK is expected to be quite rigid, while the PEG chains are expected to be more mobile. However, if the PVK and PEG are intimately mixed, their mobility is averaged, and they cannot be distinguished one from another. In Figure 6, for the samples containing 33.1 and 50.0 mol % PEG−DNB, the PEG peak was quite sharp, suggesting that the PEG chains are microphase-separated from the PVK backbone and experi-

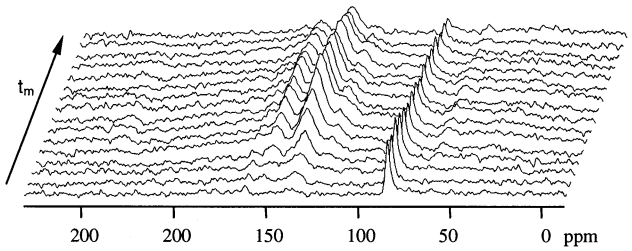

Figure 12. ^{13}C CP MAS spectra detected for PVK/PEG−DNB 33.1 mol % immediately after the dipolar filter (bottom spectrum) and after increasing mixing times (t_m).

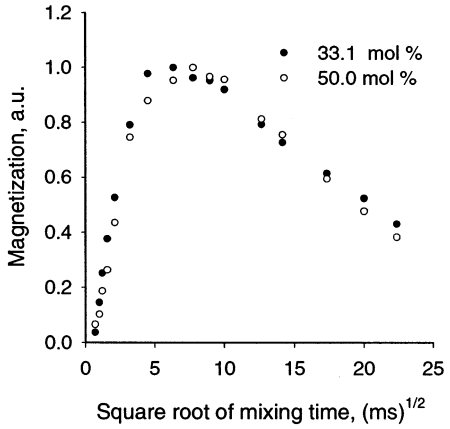

Figure 13. Spin diffusion data for two mixtures of PVK/PEG−DNB at different mol % of PEG−DNB.

ence a very mobile environment. For these samples, it was possible to use the dipolar filter to discriminate between the mobility of PVK and PEG and, consequently, to use the spin diffusion technique for domain size determination. For samples containing less PEG−DNB the dipolar filter could not be applied. In these samples the PEG chains are probably still coiled around the DNB group (Figure 7a), and their mobility is not very different from that of the PVK/DNB phase.

Figure 12 shows the ^{13}C CP MAS spectra detected immediately (100 μs) after the dipolar filter was applied (bottom spectrum) and after increasing mixing times, during which the recovery of the PVK signal can be observed. In the spectrum recorded right after the dipolar filter sequence, the PVK signal was totally suppressed. The aromatic peaks corresponding to the DNB group were also suppressed, CT complexation with carbazole making DNB part of the rigid phase.

The magnetization growth following the dipolar filter sequence can be used to estimate domain sizes. Plots of magnetization vs the square root of the mixing time can be used either to determine the spin diffusion coefficients from known domain sizes or to measure the domain sizes from known spin diffusion coefficients through simulation.[31−33] The spin diffusion curves describing the recovery of the PVK magnetization are showed in Figure 13 for the 33.1 and 50 mol % samples. The large PVK peak at 123 ppm was used to monitor the spin diffusion process. After reaching a maximum, the signal decreases at longer mixing times. This decrease is related to the spin−lattice relaxation in laboratory frame (T_1) effect and to how this effect is compensated in the pulse sequence. The spin−lattice relaxation contribution to magnetization recovery cannot be distinguished from that of spin diffusion. The phase alternation (π pulse between the dipolar filter and

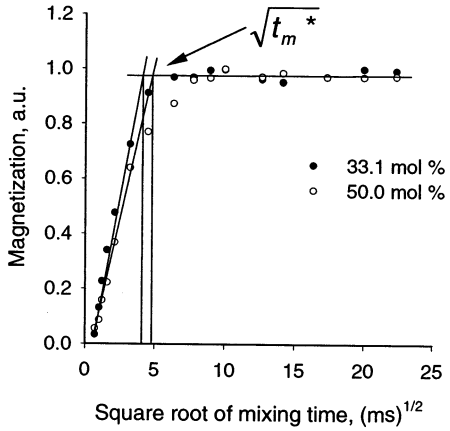

Figure 14. Corrected spin diffusion data for two mixtures of PVK/PEG−DNB at different mol % of PEG−DNB. Magnetization was corrected by exp(t_m/T_1) and normalized to the largest integral.

the mixing time at every other scan, appearing as PC in Figure 2) partially cancels the contribution of T_1 to magnetization recovery.[33] However, the application of phase cycling causes all of the observed signals to decrease in intensity at long mixing times. The reduction in the measured signal intensity is corrected by multiplying with an exponential factor, exp(t_m/T_1), where t_m is the mixing time and T_1 is the proton spin−lattice relaxation time in the laboratory frame for the resonance being measured.[34] The spin diffusion curves after T_1 correction are presented in Figure 14. The T_1 values used in the exponential factor were 450 and 530 ms for the samples containing 33.1 and 50.0 mol % PEG−DNB, respectively.

The model used to analyze spin diffusion for domain size determination assumes that the two phases exchanging magnetization are interchangeable, and it makes no difference which is the source of magnetization. If the spin diffusion coefficients for the rigid and mobile phases are known, the size of the rigid domain can be calculated using the information extracted from spin diffusion curves and the initial rate approximation:[32]

$$d_{rig} = \left(\frac{\rho_{HA}\phi_A + \rho_{HB}\phi_B}{\phi_A\phi_B}\right)\frac{4\epsilon\phi_{rig}\sqrt{D_A D_B}}{\sqrt{\pi}(\sqrt{D_A\rho_{HA}} + \sqrt{D_B\rho_{HB}})}\sqrt{t_m}^* \quad (1)$$

where ρ_H is the proton density, ϕ is the volume fraction, and D is the spin diffusion coefficient of each phase. ϵ is a parameter indicating the dimensionality of the system, thus making the equation valid for spherical ($\epsilon = 3$), cylindrical ($\epsilon = 2$), and lamellar ($\epsilon = 1$) morphologies. Subscripts A and B stand for the two phases and are interchangeable. The subscript rig stands for the rigid phase, which in this case is the PVK complexed with DNB groups. The squared root of t_m* is obtained graphically as the intersection of the extrapolations from the initial magnetization build up and equilibrium plateau (Figure 14). Values of 4.4 and 4.8 (ms)$^{1/2}$ were obtained for samples containing 33.1 and 50.0 mol % PEG−DNB, respectively. The proton densities can be easily calculated from the estimated densities and the number of protons in each phase. The spin diffusion coefficients (D_A and D_B) are unknown and need to be approximated. For amorphous poly(ethylene oxide) (PEO), using spin−spin relaxation time measurements,

Table 1. Domain Sizes for Layered Structures of PVK/PEG−DNB Obtained from Spin Diffusion Analysis

PEG−DNB (mol %)	$d_{PVK/DNB}$ (±0.5 nm)	d_{PEG} (±0.5 nm)
33.1	5.1	3.1
50.0	5.5	3.4

Mellinger et al.[53] reported values between 0.02 and 0.08 nm^2/ms for spin diffusion coefficients obtained at temperatures between 0 and 50 °C. Recently,[35] a value of 0.07 ± 0.01 nm^2/ms was estimated for amorphous PEO at 293 K, which is also the temperature at which the experiments presented here were carried out. Therefore, 0.07 ± 0.01 nm^2/ms was considered a good estimate for the diffusion coefficient of the PEG. For polymer complexes based on carbazolyl and dinitrobenzoyl moieties, a value of 0.40 nm^2/ms was estimated for the spin diffusion coefficient by simulation of intramolecular spin diffusion data.[36] Equation 1 can be used for systems in which the interfacial thickness is small with respect to the size of the domains. The presence of a significant interface thickness is usually identified by a lag in the initial magnetization buildup.[32] Spin diffusion is considered to be sensitive to microphase sizes down to 0.5 nm.[29−34] The linear fast increase in magnetization seen in Figure 14 suggests that there is a sharp separation (smaller than 0.5 nm) between the PVK and PEG phases.

Before using eq 1, the dimensionality of the system has to be established. The dimensionality of microphase-separated segmented copolymers depends on the volume fraction (ϕ) of the components. When the segmented copolymers have relatively symmetric structures (ϕ = 0.3−0.5), they form one-dimensional (lamellar) morphology, while with the increase in asymmetry, higher dimensional phase structures are obtained.[54−57] The predominant morphology that is reported for comblike polymer/surfactant complexes is lamellar, consisting of alternating layers of polymer chains separated by layers of surfactant.[6−8] A number of modifications such as undulated and perforated lamellae were also observed in some polyelectrolytes/surfactant complexes.[16−18] The PVK/PEG−DNB complexes containing 33.1 and 50.0 mol % PEG−DNB correspond to PEG (without DNB) volume fractions of 0.423 and 0.525, respectively. Considering the symmetric microphase volume fractions for PVK/DNB and PEG phases and the analogy with the polymer/surfactant systems reported in the literature,[6−8] the assumption of lamellar morphology ($\epsilon = 1$) for the spin diffusion analysis is very reasonable.

Table 1 presents the results from the analysis of the spin diffusion data for the two PVK/PEG−DNB complexes. The uncertainty of the domain sizes was estimated from two possible sources: one introduced by the choice of spin diffusion coefficients and the other from the determination of square root of t_m*. The size of the PEG microphase was determined using the equation[32]

$$d_{mob} = d_{rig}\left(\frac{1}{\sqrt[\epsilon]{\phi_{rig}} - 1}\right) \qquad (2)$$

where d_{mob} is the size of the mobile phase, PEG in this case, and all the other quantities have the same meaning as in eq 1.

To have an understanding of the estimates of domain sizes obtained from spin diffusion, it is necessary to correlate these values with the molecular sizes of the corresponding components. The size of the PEG microdomains is related to the root-mean-square end-to-end distance, $\langle r^2\rangle^{1/2}$, of the PEG chains, which is about 1.9 nm as calculated using Flory equation.[58] The values obtained for the thickness of the PEG phase is about twice the end-to-end distance of the PEG chain, suggesting a bilayer structure for this phase (Figure 15), similar to the surfactant structure reported in polyeletrolyte/surfactant complexes.[6−8] The high average molecular weight (10^6 g/mol) of the PVK chains is expected to give a large value for $\langle r^2\rangle^{1/2}$, about 60 nm as calculated from the same Flory equation.[58] This value is too large compared with the domain size determined from NMR. The PVK chain must be oriented perpendicular to the direction of the domain thickness in the layer plane (Figure 15). This means that the molecular size that has to be correlated to the thickness of the PVK phase is the width of the chain and not its length. Molecular simulation of the conformational arrangements of the PVK chains performed on heptads indicated that chain thickness is about 1.5 nm.[59] The coplanar sandwich geometry of the carbazole/DNB complex[38,43] is not expected to affect significantly the thickness of the PVK chains. Comparing the PVK microdomain size determined by spin diffusion (Table 1) with the size of a PVK chain suggests that the thickness of the PVK/DNB layer is given by more than one chain, most likely between two and three (Figure 15). Undulation and folding along the PVK chain may also result in higher effective thickness of the PVK/DNB microdomain. Finally, a comparison between the domain sizes of the two polymer complexes cannot be made since the differences are not significant, being smaller than the measurement error (Table 1).

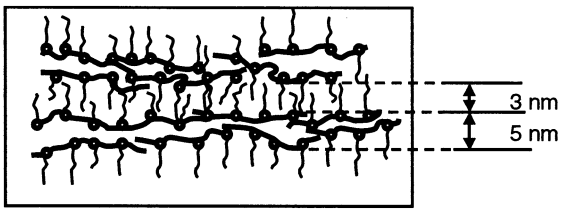

Figure 15. Schematic representation of the layered structure in the PVK/PEG−DNB comblike complexes.

Conclusions

Macromolecular CT complexes between PVK and PEG−DNB were investigated for their potential to form comblike architectures in a manner similar to polyelectrolyte/ surfactant complexes. PVK and PEG−DNB are homogeneously mixed in these complexes down to the level detected by T_g and $T_{1\rho}$(H). For samples containing 33.1 and 50.0 mol % PEG−DNB, the microphase separation between the PEG and PVK chains is first suggested by the PEG sharp peaks observed in ^{13}C CP MAS NMR spectra and then confirmed by the analysis of spin diffusion data. This microphase separation is the result of the balance between the repulsion forces associated with the incompatibility of the PVK and PEG phases, on one side, and the binding forces provided by the CT complexation between carbazole and DNB groups, on the other. In the samples where microphase separation was observed, the volume fraction of the PEG phase was about 0.4−0.5. At these symmetric ratios, the entropy of mixing is low while the positive enthalpy of mixing between the PVK and PEG chains is high and so is their tendency to phase-separate. At small concentrations of surfactant, the unfavorable enthalpy of

mixing between PVK and PEG chains is too small to induce microphase separation and is overcome by entropy. In these samples, the PEG chains were observed to experience increased rigidity, suggesting that they are intimately mixed with the PVK chains, sharing their rigid environment. The PEG chains are probably still coiled around the DNB group, which is itself complexed to the rigid carbazole groups.

Based on the analysis of spin diffusion data, estimates for the microdomain sizes were obtained. The size of the PEG microdomain is about twice the mean end-to-end distance of the PEG chains, suggesting a bilayer structure in the PEG microphase. This type of structure is common for the microphase formed by surfactant chains in polyelectrolyte/surfactant complexes.[6−8] The PVK microphase is formed by layers whose thickness correspond to about two PVK/DNB complexed backbones.

Acknowledgment. We thank NSERC Canada for financial support. G.C. acknowledges the PGS B Scholarship granted by NSERC.

References and Notes

(1) Förster, S.; Antonietti, M. *Adv. Mater.* **1998**, *10*, 195.
(2) Stupp, S. I.; LeBonheur, V.; Walker, K.; Li, L. S.; Huggins, K. E.; Keser, M.; Amstutz, A. *Science* **1997**, *276*, 384.
(3) Hasegawa, H.; Hashimoto, T. In *Comprehensive Polymer Science*, 2nd Suppl.; Aggarwal, S. L., Russo, S., Eds.; Pergamon: London, 1994.
(4) ten Brinke, G.; Ikkala, O. *Trends Polym. Sci.* **1997**, *5*, 213.
(5) Harada, A.; Nozakura, S. *Polym. Bull. (Berlin)* **1984**, *11*, 175.
(6) Antonietti, M.; Burger, C.; Thünemann, A. *Trends Polym. Sci.* **1997**, *5*, 262.
(7) Ober, C. K.; Wegner, G. *Adv. Mater.* **1997**, *9*, 17.
(8) Macknight, W. J.; Ponomarenko, E. A.; Tirrell, D. A. *Acc. Chem. Res.* **1998**, *31*, 781.
(9) Ruokolainen, J.; Mäkinen, R.; Torkkeli, M.; Mäkelä, T.; Serimaa, R.; ten Brinke, G.; Ikkala, O. *Science* **1998**, *280*, 557.
(10) Polushkin, E.; Alberda van Ekenstein, G. O. R.; Knaapila, M.; Ruokolainen, J.; Torkkeli, M.; Serimaa, R.; Bras, W.; Dolbnya, I.; Ikkala, O.; ten Brinke, G. *Macromolecules* **2001**, *34*, 4917.
(11) De Moel, K.; Alberda van Ekenstein, G. O. R.; Nijland, H.; Polushkin, E.; ten Brinke, G. *Chem. Mater.* **2001**, *13*, 4580.
(12) Dormidontova, E.; ten Brinke, G. *Colloids Surf. A*: *Physicochem. Eng. Aspects* **1999**, *147*, 249.
(13) Zhou, S.; Hu, H.; Burger, C.; Chu, B. *Macromolecules* **2001**, *34*, 1772.
(14) Jiao, H.; Goh, S. H.; Valiyaveettil, S. *Macromolecules* **2001**, *34*, 7162.
(15) Chen, L.-H.; Hsiao, M.-S. *Macromolecules* **1999**, *32*, 2967.
(16) Antonietti, M.; Radloff, D.; Wiesner, U.; Spiess, H. W. *Macromol. Chem. Phys.* **1996**, *197*, 2713.
(17) Antonietti, M.; Wenzel, A.; Thünemann, A. *Langmuir* **1996**, *12*, 2111.
(18) Antonietti, M.; Maskos, M. *Macromolecules* **1996**, *29*, 4199.
(19) Ruokolainen, J.; Tanner, J.; ten Brinke, G.; Ikkala, O.; Torkkeli, M.; Serimaa, R. *Macromolecules* **1995**, *28*, 7779.
(20) Hartikainen, J.; Lahtinen, M.; Torkkeli, M.; Serimaa, R.; Valkonen, J.; Rissanen, K.; Ikkala, O. *Macromolecules* **2001**, *34*, 7789.
(21) Foster, R.; Fyfe, C. A. *Prog. Nucl. Magn. Reson. Spectrosc.* **1969**, *4*, 1.
(22) Foster, R. *Organic Charge-Transfer Complexes*; Academic Press: London, 1969.
(23) Rodriguez-Parada, J. M.; Percec, V. *Macromolecules* **1986**, *19*, 55.
(24) Clark, J. N.; Higgins, J. S.; Peiffer, D. G. *Polym. Eng. Sci.* **1992**, *32*, 49.
(25) Cojocariu, G.; Natansohn, A. *Macromolecules* **2001**, *34*, 3827.
(26) Cojocariu, G.; Natansohn, A. *J. Phys. Chem. B* **2002**, *106*, 11737.
(27) Stejskal, E. O.; Schaefer, J.; Sefcik, M. D.; McKay, R. A. *Macromolecules* **1981**, *14*, 275.
(28) McBrierty, V. J. In *Comprehensive Polymer Science*; Allen, G., Ed.; Pergamon Press: Oxford, 1989; Vol. 1, p 397.
(29) Schmidt-Rohr, K.; Clauss, J.; Blümich, B.; Spiess, H. W. *Magn. Reson. Chem.* **1990**, *38*, 3.
(30) Clauss, J.; Schmidt-Rohr, K.; Adam, A.; Boeffel, C.; Spiess, H. W. *Macromolecules* **1992**, *25*, 5208.
(31) Cai, W. Z.; Spiegel, S.; Schmidt-Rohr, K.; Egger, N.; Gerhartz, B.; Spiess, H. W. *Polymer* **1993**, *34*, 267.
(32) Clauss, J.; Schmidt-Rohr, K.; Spiess, H. W. *Acta Polym.* **1993**, *44*, 1.
(33) Schmidt-Rohr, K.; Spiess, H. W. *Multidimensional Solid State NMR and Polymers*; Academic Press: London, 1994.
(34) Spiegel, S.; Schmidt-Rohr, K.; Boeffel, C.; Spiess, H. W. *Polymer* **1993**, *34*, 4566.
(35) Yu, H.; Natansohn, A.; Singh, M. A.; Torriani, I. *Macromolecules* **2001**, *34*, 1258.
(36) Cho, G.; Natansohn, A. *Chem. Mater.* **1997**, *9*, 148.
(37) Natansohn, A. *Polym. Eng. Sci.* **1992**, *32*, 1711.
(38) Simmons, A.; Natansohn, A. *Macromolecules* **1991**, *24*, 3651.
(39) Simmons, A.; Natansohn, A. *Macromolecules* **1992**, *25*, 1272.
(40) Piton, M. C.; Natansohn, A. *Macromolecules* **1995**, *28*, 1598.
(41) Kaplan, D. S. *J. Appl. Polym. Sci.* **1976**, *20*, 2615.
(42) Olabisi, O.; Robeson, L. M.; Shaw, M. T. *Polymer−Polymer Miscibility*; Academic Press: New York, 1979.
(43) Cojocariu, G.; Natansohn, A. Submitted to *J. Phys. Chem. B*.
(44) Huang, X. D.; Goh, S. H.; Lee, S. Y.; Zhao, Z. D.; Wong, M. W.; Huan, C. H. A. *Macromolecules* **1999**, *32*, 4327.
(45) Jiang, X. Z.; Register, R. A.; Killeen, K. A.; Thompson, M. E.; Pschenitzka, F.; Sturm, J. C. *Chem. Mater.* **2000**, *12*, 2542.
(46) Karlou, K.; Schneider, H. A. *J. Therm. Anal. Calorim.* **2000**, *59*, 59.
(47) Feldstein, M. M.; Shandryuk, G. A.; Kuptsov, S. A.; Plate, N. A. *Polymer* **2000**, *41*, 5327.
(48) Feldstein, M. M.; Shandryuk, G. A.; Plate, N. A. *Polymer* **2001**, *42*, 971.
(49) Feldstein, M. M.; Kuptsov, S. A.; Shandryuk, G. A.; Plate, N. A. *Polymer* **2001**, *42*, 981.
(50) Feldstein, M. M.; Lebedeva, T. L.; Shandryuk, G. A.; Kotomin, S. V.; Kuptsov, S. A.; Igonin, V. E.; Grokhovskaya, T. E.; Kulichikhin, V. G. *J. Polym. Sci.* **1999**, *41*, 854.
(51) Cesteros, L. C.; Quintana, J. R.; Fernandez, J. A.; Katime, I. *J. Polym. Sci., Polym. Phys. Ed.* **1989**, *27*, 2567.
(52) Bloembergen, N.; Purcell, E. M.; Pound, R. V. *Phys. Rev.* **1948**, *73*, 679.
(53) Mellinger, F.; Wilhelm, M.; Spiess, H. W. *Macromolecules* **1999**, *32*, 4686.
(54) Bates, F. S.; Fredrickson, G. H. *Annu. Rev. Phys. Chem.* **1990**, *41*, 525.
(55) Bates, F. S.; Schultz, M. F.; Khandpur, A. K.; Förster, S.; Rosedale, J. H.; Almdal, K.; Mortensen, K. *Faraday Discuss. Chem. Soc.* **1994**, *98*, 7.
(56) Matsen, M. W.; Bates, F. S. *Macromolecules* **1996**, *29*, 7641.
(57) Matsen, M. W.; Bates, F. S. *J. Chem. Phys.* **1997**, *106*, 2436.
(58) Flory, P. J. *J. Am. Chem. Soc.* **1952**, *74*, 3364.
(59) Karali, A.; Froudakis, G. E.; Dais, P.; Heatley, F. *Macromolecules* **2000**, *33*, 3180.

MA026012H